

Tuning and Dissecting Electronic and Steric Effects in Ammonium Receptors: Nonactin vs Artificial Receptors

Jik Chin,^{*,†} Jinho Oh,[‡] Sang Yong Jon,[‡] Sang Hyun Park,[‡] Christian Walsdorff,[‡]
Brent Stranix,[†] Assaad Ghossoub,[†] Seok Jong Lee,[†] Hyun Jei Chung,[‡]
Su-Moon Park,^{*,‡} and Kimoon Kim^{*,‡}

Contribution from the Department of Chemistry, University of Toronto, 80 St. George Street, Toronto, Ontario, Canada M5S 1A1, National Creative Research Initiative Center for Smart Supramolecules, Center for Integrated Molecular Systems, and Department of Chemistry, Division of Molecular and Life Sciences, Pohang University of Science and Technology, San 31 Hyojadong, Pohang 790-784, Republic of Korea

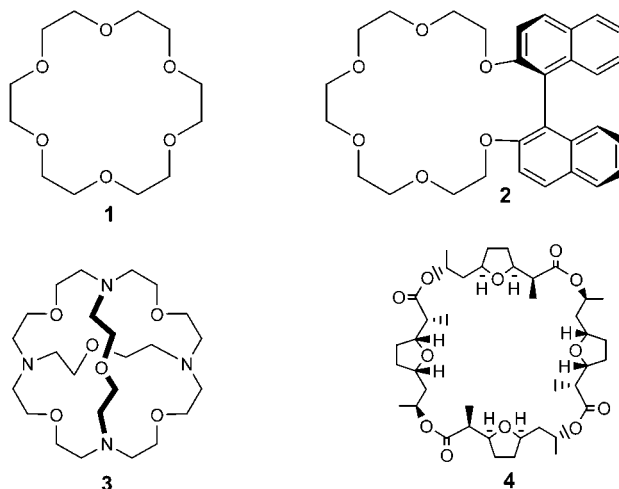
Received October 29, 2001

Abstract: Ion selective electrodes (ISE) based on three different tripodal receptors (**5**, **6**, and **7**) have been investigated for sensing ammonium ion. Each receptor is based on three pyrazole groups that can accept three H-bonds from the bound ammonium ion. The receptor based on 4-bromo-3,5-dimethylpyrazole (**6**) is the most sensitive with a detection limit for ammonium ion of 2.5×10^{-5} M at pH 8. The detection limits for the receptors based on 2,3-dimethylpyrazole (**5**) and unsubstituted pyrazole (**7**) are 1.0×10^{-4} and 2.0×10^{-4} M, respectively. The selectivities of the receptors **5**, **6**, and **7** for sensing ammonium ion over potassium ion ($\log K_{\text{NH}_4^+/\text{K}^+}$) are -2.8 , -2.3 , and -1.7 , respectively. In contrast, the detection limit and the selectivity of a nonactin-based ISE are 2.2×10^{-5} M and -1.3 , respectively. Crystallographic studies reveal that **6** accepts three H-bonds from the bound ammonium and singly protonated receptor **5** forms three H-bonds with the bound water molecule.

Introduction

The study of ammonium ion recognition is of considerable fundamental and practical interest. It is also central to the understanding of chiral and achiral alkylammonium recognition (e.g., amino acids and the dopamine class of neurotransmitters).¹ The early finding that 18-crown-6 (**1**)² is an excellent receptor for NH_4^+ led to the development of chiral analogues (**2**)³ for stereospecific recognition of alkylammonium ions (Chart 1). A cryptand (**3**)⁴ has been shown to be even better than crown ethers for binding NH_4^+ . Nonactin (**4**), a naturally occurring antibiotic that binds tightly to NH_4^+ , is currently used in commercial ion selective electrodes (ISEs) for detecting the cation down to micromolar levels.⁵ Such sensors are useful for indirectly measuring the concentrations of urea or creatine in biological samples,⁶ as well as for directly measuring the concentrations of NH_4^+ in the environment.⁷ A major problem with nonactin-

Chart 1



based ISEs is that although they are highly sensitive, their selectivity for binding NH_4^+ over K^+ is low.

In a recent communication, we showed that **5** is over 10 times more selective than nonactin for binding NH_4^+ over K^+ .⁸ Since K^+ prefers to be coordinated by six or more atoms, we have been able to increase the selectivity by lowering the number of coordinating atoms in the receptor from eight in nonactin (**4**) to three in **5**. However, this approach led to a drastic reduction

* Corresponding author. E-mail: jchin@chem.utoronto.ca.

[†] University of Toronto.

[‡] Pohang University of Science and Technology.

(1) Zhang, X. X.; Bradshaw, J. S.; Izatt, R. M. *Chem. Rev.* **1997**, *97*, 3313–3361.

(2) Pedersen, C. J. *J. Am. Chem. Soc.* **1967**, *89*, 7017–7036.

(3) Cram, D. J. *Science* **1988**, *240*, 760–767.

(4) Lehn, J. M. *Acc. Chem. Res.* **1978**, *11*, 49–57.

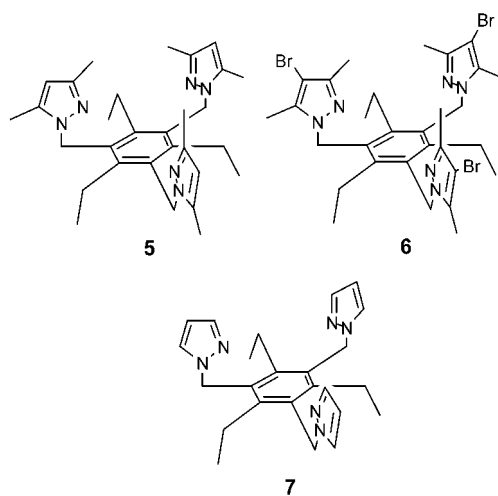
(5) Young, C. C. *J. Chem. Educ.* **1997**, *74*, 177–182. Ghauri, M. S.; Thomas, J. S. R. *Analyst* **1994**, *119*, 2323–2326. Beer, D. De.; van den Heuvel, J. C. *Talanta* **1988**, *35*, 728–730. Davies, O. G.; Moody, G. J.; Thomas, J. D. R. *Analyst* **1988**, *113*, 497–500. Ma, S. C.; Chaniotakis, N. A. Meyerhoff, M. E. *Anal. Chem.* **1988**, *60*, 2293–2299.

(6) Wolfbeis, O. S.; Li, H. *Biosens. Bioelectron.* **1993**, *8*, 161–166.

(7) Buhlman, P.; Pretsch, E.; Bakker, E. *Chem. Rev.* **1998**, *98*, 1593–1689.

(8) Chin, J.; Walsdorff, C.; Stranix, B.; Oh, J.; Chung, H. J.; Park, S.-M.; Kim, K. *Angew. Chem., Int. Ed. Engl.* **1999**, *38*, 2756–2759.

Chart 2



in the sensitivity of the receptor for detecting NH_4^+ at neutral pH. Here we investigate how steric and electronic effects influence the selectivity and sensitivity of the receptors by comparing the performances of ISEs based on **5**, **6**, and **7** (Chart 2). We also report the effect of solution pH on the sensitivity of the receptors for detecting NH_4^+ .

Experimental Section

Instruments. ^1H NMR and ^{13}C NMR spectra were recorded on Bruker DPX 300 and DRX 500 NMR spectrometers at room temperature. Chemical shifts are reported in ppm with tetramethylsilane used as reference.

Materials. All commercially available reagents were purchased from Aldrich or Fluka and used without further purification. Tetrahydrofuran was dried by distillation from sodium metal.

Compound 5: To a suspension of NaH (0.62 g, 16 mmol) in 40 mL of anhydrous THF was added 3,5-dimethylpyrazole (1.48 g, 16 mmol) in small portions at room temperature. The mixture was stirred for 20 min until the evolution of hydrogen gas ceased. The resulting solution was slowly added to a slurry of 1,3,5-tris(bromomethyl)-2,4,6-triethylbenzene (2.0 g, 4.6 mmol) in 20 mL of anhydrous THF. After being stirred for 3 h, the mixture was poured into water (50 mL) and extracted with CH_2Cl_2 (50 mL \times 2). The combined organic extract was dried over MgSO_4 and evaporated under reduced pressure. The remaining solid was washed with ether to remove excess 3,5-dimethylpyrazole and dried in vacuo to give 1.62 g (73%) of the product as colorless crystals. ^1H NMR (CDCl_3 , 300 MHz) δ 0.86 (9 H, t, Me), 2.14 (9 H, s, Me), 2.15 (9 H, s, Me), 2.77 (6 H, q, CH_2), 5.18 (6 H, s, CH_2), 5.76 (3 H, s, pyrazol-4-yl-H); ^{13}C NMR (CDCl_3 , 75 MHz) δ 11.85, 13.75, 15.09, 24.12, 47.59, 106.03, 130.83, 139.85, 145.62, 147.38. Anal. Calcd for $\text{C}_{30}\text{H}_{42}\text{N}_6$: C, 74.03; H, 8.70; N, 17.27. Found: C, 73.79; H, 8.71; N, 17.04.

Compound 6: To a solution of **5** (1.0 g, 2.1 mmol) in CHCl_3 was slowly added Br_2 (0.42 mL, 8.2 mmol) at 0 °C. The reaction mixture was stirred for 1 h and poured into a saturated solution of K_2CO_3 (50 mL) and extracted with CHCl_3 (30 mL \times 2). The extracts were evaporated to give 1.43 g (97%) of the product as a yellow solid. ^1H NMR (CDCl_3 , 300 MHz) δ 5.16 (6H, s, CH_2), 2.68 (6H, q, CH_2), 2.10 (18H, d, CH_3), 0.86 (9H, t, CH_3); ^{13}C NMR (CDCl_3 , 75 MHz) δ 146.38, 145.82, 137.47, 130.37, 94.91, 48.26, 24.12, 15.08, 12.70, 10.94. FAB-MS m/z 721 ($\text{M} + 1$)⁺. Anal. Calcd for $\text{C}_{30}\text{H}_{39}\text{Br}_3\text{N}_6$: C, 49.81; H, 5.43; N, 11.62. Found: C, 49.65; H, 5.51; N, 11.62.

Compound 7: The product was obtained as colorless crystals in 65% yield following the same general procedure for making **5**. ^1H NMR (CDCl_3 , 300 MHz) δ 7.48 (3H, d, pyrazol-5-yl-H), 6.95 (3H, d, pyrazol-5-yl-H), 6.15 (3H, t, pyrazol-4-yl-H), 5.39 (6H, s, CH_2), 2.66

Table 1. Crystal and Structure Refinement Data for $[\text{5H}^+\cdot\text{H}_2\text{O}] \text{ClO}_4^-$ and $[\text{6}\cdot\text{NH}_4] \text{PF}_6^-$

	$[\text{5H}^+\cdot\text{H}_2\text{O}] \text{ClO}_4^-$	$[\text{6}\cdot\text{NH}_4] \text{PF}_6^-$
empirical formula	$\text{C}_{30}\text{H}_{43}\text{Br}_3\text{F}_6\text{N}_7\text{P}$	$\text{C}_{30}\text{H}_{43}\text{Br}_3\text{F}_6\text{N}_7\text{P}$
formula wt	605.17	886.41
crystal size, mm ³	$0.6 \times 0.5 \times 0.4$	$0.40 \times 0.40 \times 0.25$
crystal system	monoclinic	triclinic
space group	$P2_1/c$	$P\bar{1}$
temp, K	188(2)	243(2)
<i>a</i> , Å	8.9653(1)	10.8201(2)
<i>b</i> , Å	19.4149(3)	11.8525(3)
<i>c</i> , Å	18.4104(2)	16.0993(1)
α , deg	90	93.654(1)
β , deg	90.086(1)	98.994(1)
γ , deg	90	113.193(1)
vol, Å ³	3204.52(7)	1856.53
Z	4	2
<i>d</i> _{calc} , g/cm ³	1.254	1.586
μ , mm ⁻¹	0.166	3.364
no. of reflns collected	12615	7581
no. of unique reflns	4967	5567
no. of variables	403	428
R1, wR2, %	4.45, 12.23	5.92, 15.49
goodness of fit	0.764	1.055

^a All the data were collected on a SMART CCD diffractometer with Mo K α radiation ($\lambda = 0.71071$ Å).

(6H, q, CH_2), 0.90 (9H, t); ^{13}C NMR (75 MHz, CDCl_3) δ 146.44, 139.67, 130.81, 128.31, 105.99, 49.96, 23.70, 15.58.

Complex $[\text{6}\cdot\text{NH}_4] \text{PF}_6^-$: The complex was generated by mixing equimolar quantities of **6** and NH_4PF_6 in $\text{CH}_3\text{CN}/\text{CHCl}_3$ (1:1 v/v). ^1H NMR (CDCl_3 , 300 MHz) δ 6.60(4H, br), 5.17(6H, s, CH_2), 2.50(6H, br, CH_2), 2.30(9H, br, CH_3), 2.11(9H, br, CH_3), 1.23(9H, br, CH_3); FAB-MS m/z 739 (M^+). Anal. Calcd for $\text{C}_{30}\text{H}_{45}\text{Br}_3\text{F}_6\text{N}_7\text{OP}$: C, 39.84; H, 5.02, N, 10.84. Found: C, 39.79; H, 4.82; N, 10.75.

Complex $[\text{5H}^+\cdot\text{H}_2\text{O}] \text{ClO}_4^-$: The complex was obtained as a white powder by adding perchloric acid to a solution of **5** dissolved in dilute hydrochloric acid. Recrystallization of the white powder from ethanol gave colorless rectangular plates of the product. ^1H NMR (CD_3OD , 500 MHz) δ 6.20(3H, s, pyrazol-4-yl-H), 5.39 (6H, s, CH_2), 2.67 (6H, q, CH_2), 2.51 (9H, s, CH_3), 2.20 (9H, s, CH_3), 0.95 (9H, t, CH_3); ^{13}C NMR (125 MHz, CD_3OD) δ 147.86, 147.31, 143.66, 129.32, 107.06, 46.45, 23.59, 14.06, 11.13, 10.42. Anal. Calcd for $\text{C}_{30}\text{H}_{45}\text{ClN}_6\text{O}$: C, 59.54; H, 7.49, N, 13.89. Found: C, 59.13; H, 7.46; N, 13.75.

Crystallography. The intensity data for $[\text{5H}^+\cdot\text{H}_2\text{O}] \text{ClO}_4^-$ and $[\text{6}\cdot\text{NH}_4] \text{PF}_6^-$ were collected using a Siemens diffractometer equipped with a graphite-monochromated Mo K α ($\lambda = 0.71073$ Å) radiation source and a CCD detector. The structures were solved by pattern synthesis (SHELXLS86) and subsequent difference Fourier methods (SHELXL93). Calculations were performed with the SHLXTL v5.1 program.⁹ Semiempirical absorption corrections were not applied for the structures. All the nonhydrogen atoms were refined anisotropically. While most hydrogen atoms of the complex $[\text{5H}^+\cdot\text{H}_2\text{O}] \text{ClO}_4^-$ were generated with ideal geometry, the hydrogen atoms around water (H1, H2, and H3) were located from difference Fourier maps and refined without any constraints. Crystal and structure refinement data for $[\text{5H}^+\cdot\text{H}_2\text{O}] \text{ClO}_4^-$ and $[\text{6}\cdot\text{NH}_4] \text{PF}_6^-$ are summarized in Table 1. H-bonding interactions are listed in Tables 2 and 3. The illustrations of the two crystal structures prepared by using the ORTEP¹⁰ program are shown in Figures 1 and 2.

General Procedure for Preparation of Ion Selective Electrodes and Measurement of Their Performances. The ionophore (1 mg), PVC (33 mg), and bis(2-ethylhexyl)adipate (DOA as a plasticizer, 66 mg) were dissolved in anhydrous THF. The mixture was vigorously

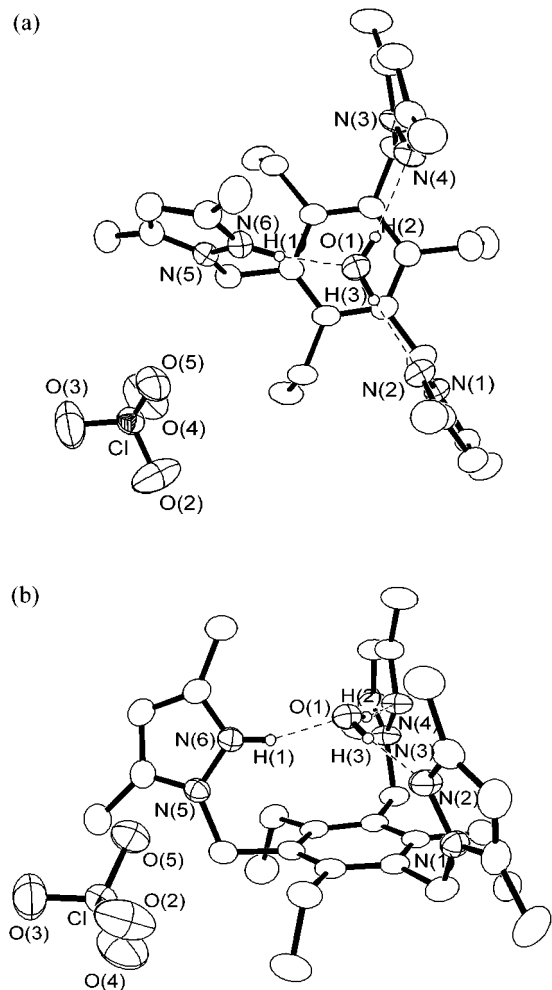
(9) *SHELXTL* v5.1 from Bruker-AXS, Inc.: Madison, WI, 1998.
 (10) *ORTEP*: Johnson, C. K. 1976. ORTEP-A Fortran Thermal Ellipsoid Plot Program; Technical Report ORNL-5138; Oak Ridge National Laboratory: Oak Ridge, TN, 1976.

Table 2. Selected Distances(Å) and Angles (deg) for $[5\text{H}^+\cdot\text{H}_2\text{O}]\text{ClO}_4^-$

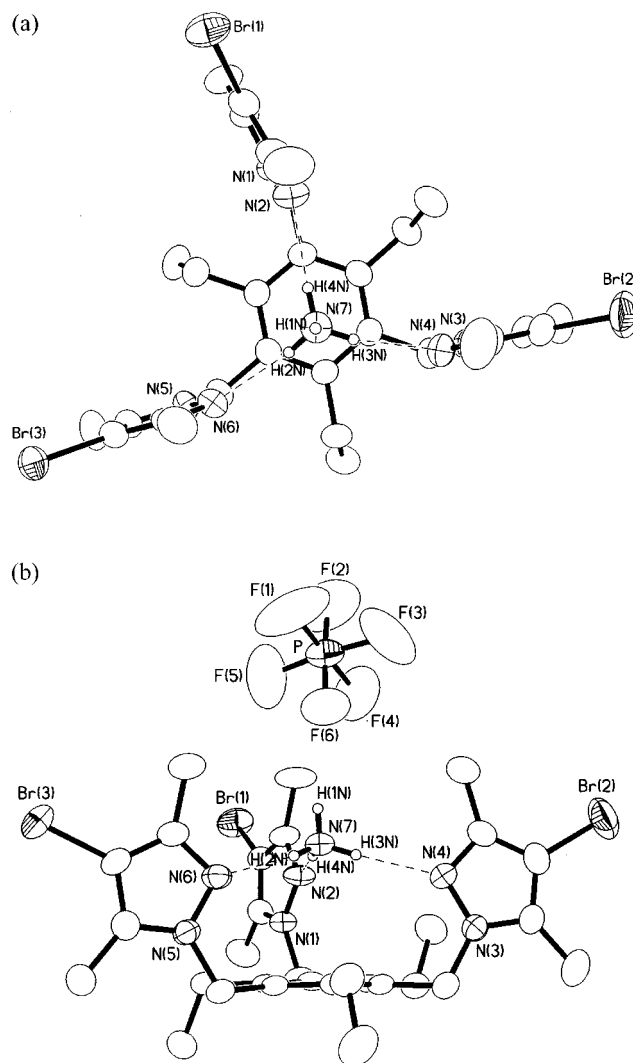
bond distances			
O(1)–H(1)	1.78 (3)	O(1)–H(2)	0.84 (3)
O(1)–H(3)	0.88 (3)	H(2)–N(4)	2.07 (3)
H(3)–N(2)	2.01 (3)	H(1)–N(6)	0.92 (3)
O(1)–O(5)	5.47 (1)	O(5)–N(6)	3.85 (2)
N(6)–O(1)	2.67 (2)	N(4)–O(1)	2.89 (3)
N(6)–O(5)	3.85 (3)		
bond angles			
O(1)–H(2)–N(4)	167 (3)	O(1)–H(3)–N(2)	174 (3)
O(1)–H(1)–N(6)	163 (2)		

Table 3. Selected Distances(Å) and Angles (deg) for $[6\cdot\text{NH}_4^+]\text{PF}_6^-$

bond distances			
N(7)–H(1)	0.85 (7)	N(7)–H(2)	0.83 (7)
N(7)–H(3)	0.92 (8)	N(7)–H(4)	0.90 (8)
H(1)–F(6)	2.37 (7)	H(2)–N(6)	2.09 (8)
H(3)–N(4)	2.02 (8)	H(4)–N(2)	2.10 (8)
N(7)–F(6)	3.18 (1)	N(7)–N(2)	2.99 (1)
N(7)–N(4)	2.92 (1)	N(7)–N(6)	2.91 (1)
bond angles			
N(7)–H(1)–F(6)	159 (5)	N(7)–H(4)–N(2)	171 (6)
N(7)–H(3)–N(4)	165 (6)	N(7)–H(2)–N(6)	167 (6)

**Figure 1.** Structure of $[5\text{H}^+\cdot\text{H}_2\text{O}]\text{ClO}_4^-$ ((a) top and (b) side views) with the thermal ellipsoids set at the 50% probability level.

stirred for 6 h. The resulting solution was poured into a glass ring (i.d. 22 mm) on a glass slide and dried over a day at room temperature. Small disks were punched from the cast films and mounted on Philips

**Figure 2.** Structure of $[6\cdot\text{NH}_4^+]\text{PF}_6^-$ ((a) top and (b) side views) with the thermal ellipsoids set at the 50% probability level.

electrode bodies (IS-561). Each electrode was filled with an ammonium chloride solution (0.01 M) as an internal reference soaked in distilled water for 12 h before use. Potential differences between the ISEs and the Orion sleeve-type double junction Ag/AgCl reference electrode (Model 90-02) were recorded using an IBM AT-type computer equipped with a 16 channel analog-to-digital converter. The dynamic response curves were obtained at room temperature by adding standard solutions of ammonium chloride or potassium chloride to 200 mL of water (0.05 M Tris-HCl buffer, pH 7.2, 8.0, and 9.0, respectively) every 100 s to vary the concentrations of each ionic species stepwise (Figure 3). The potentials were measured every second at room temperature. Selectivity coefficients were estimated according to the fixed interference method (FIM, 0.1 M interference ion).¹¹

Results and Discussion

In designing novel receptors, much can be learned from the studies of nonactin. Crystallographic studies showed that NH_4^+ or K^+ is positioned at the center of a cube formed from the four ether oxygens and the four carbonyl oxygens of nonactin (4).^{12,13} The average distance between the eight oxygen atoms

(11) Umezawa, Y.; Umezawa, K.; Sato, H. *Pure Appl. Chem.* **1995**, *67*, 507–518.

(12) Neupert-Laves, K.; Dobler, M. *Helv. Chim. Acta* **1976**, *59*, 614–623.

(13) Dobler, M.; Dunitz, J. D.; Kilburn, B. T. *Helv. Chim. Acta* **1969**, *52*, 2573–2583.

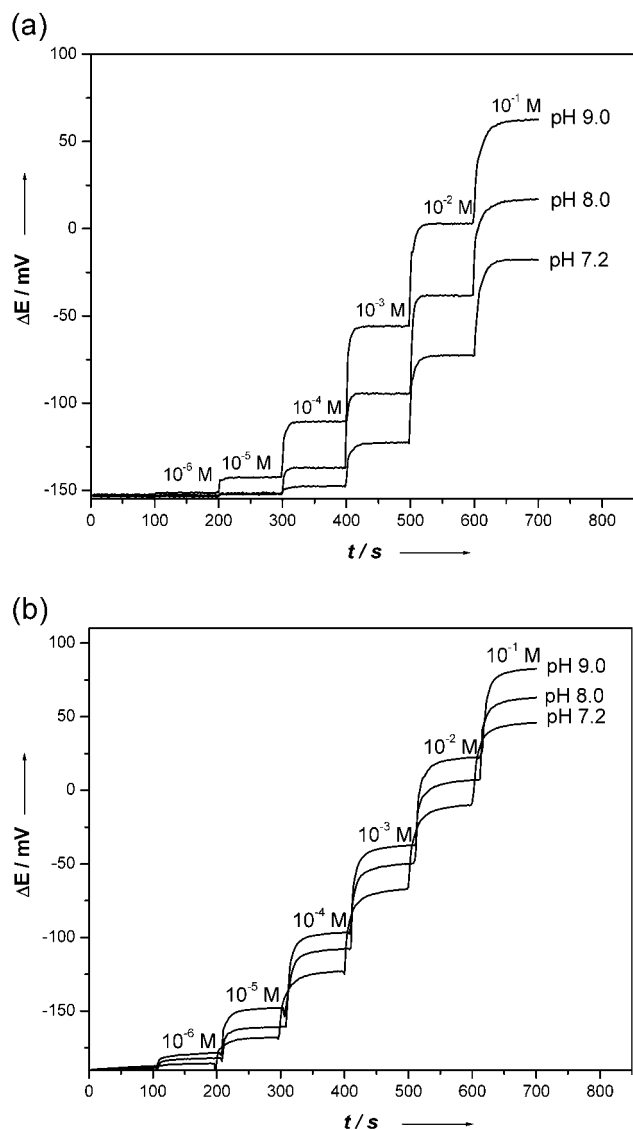
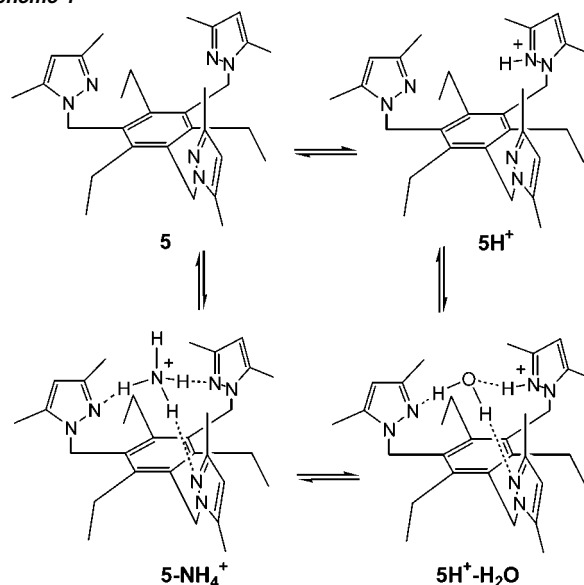


Figure 3. The ISE responses of (a) **6** and (b) nonctin for NH_4^+ at various pH values (7.2, 8.0, and 9.0).

of the receptor and the cationic center is 2.97 and 2.81 Å for NH_4^+ and K^+ , respectively. Four of the nonactin ether oxygens form H-bonds with NH_4^+ while the four carbonyl oxygens appear to stabilize the cation by dipole interactions. In contrast, all eight oxygens of nonactin coordinate to K^+ . The high sensitivity of nonactin for binding NH_4^+ and K^+ is likely due to the multidentate nature of the receptor and the low selectivity due to the comparable size and charge of the two cations.

It is well-known that K^+ prefers to be coordinated by six or more atoms.¹⁴ Thus, lowering the number of coordinating groups from eight in nonactin to three in **5** has led to a receptor with greater selectivity for binding NH_4^+ over K^+ . However, this has also resulted in significantly lowering the sensitivity of the receptor for binding NH_4^+ . One reason for the lowered sensitivity may be due to binding of water to the singly protonated form of the receptor. Figure 1 shows the crystal structure of H_2O bound to **5H⁺** (**5H⁺**· H_2O , Scheme 1). This structure is analogous to that of NH_4^+ bound to **5** (**5**· NH_4^+ , Scheme 1).⁸ The three pyrazole rings converge to form three

Scheme 1



H-bonds with the bound H_2O molecule while the three ethyl groups point to the opposite side as expected from molecular mechanics computations.^{15,16}

Figure 2 shows the crystal structure of NH_4^+ bound to **6**. It is interesting to compare the NH_4^+ and H_2O bound structures (Figures 1 and 2). In binding NH_4^+ , the neutral receptor (**6**) accepts three H-bonds with $\text{N}\cdots\text{H}$ distances of 2.02(8), 2.09(8), and 2.10(8) Å. In contrast, the singly protonated receptor (**5H⁺**) accepts two H-bonds from the bound H_2O and donates one H-bond to it. The crystal structure (Figure 1) shows that one of the three hydrogens involved in the H-bonding is located closer to the pyrazole nitrogen (0.92(3) Å) than to the water oxygen (1.78(3) Å) while the other two are positioned closer to the water oxygen (0.88(3), 0.84(3) Å) than to the pyrazole nitrogens (2.01(3), 2.07(3) Å). The reason the positions of the three hydrogens are not averaged or disordered appears to be due to the positioning of the counteranion close to the protonated pyrazole. Another difference between the bound NH_4^+ and the bound H_2O is that the former can donate a H-bond to the counteranion but the latter can only accept a H-bond. Consistent with this interpretation, the perchlorate counteranion is far removed from the bound H_2O (Figure 1: $\text{O}\cdots\text{O}$ distance of 5.47(1) Å) while the pentafluorophosphate counteranion is within H-bonding distance of the bound NH_4^+ (Figure 2: $\text{N}\cdots\text{F}$ distance of 3.18(1) Å). This difference in the H-bonding property of the bound NH_4^+ and the bound H_2O could perhaps be used to develop receptors that are highly selective for binding NH_4^+ over H_2O . Finally, cation- π interaction¹⁷ between the benzene ring of the receptor and the guest molecule may be weaker in the H_2O bound complex relative to that in the NH_4^+ bound complex since the bound water oxygen is not positively charged as in the bound ammonium nitrogen.

Two simple approaches can be used to lower the binding of water and thus increase the sensitivity of the receptor. First, placing electron withdrawing groups on the pyrazole rings of

(14) Wilkins, G.; Gillard, R. D.; McCleverty, J. A. *Comprehensive Coordination Chemistry*; Pergamon Press: New York, 1987; Vol. 3, p 3.

(15) Iverson, D. J.; Hunter, G.; Blount, J. F.; Damewood, J. R.; Mislow, K. J. *J. Am. Chem. Soc.* **1981**, *103*, 6073–6083.

(16) Bisson, A. P.; Lynch, V. M.; Monahan, M.-C. K.; Anslyn, E. V. *Angew. Chem., Int. Ed. Engl.* **1997**, *36*, 2340–2342.

(17) Dougherty, D. A. *Science* **1996**, *271*, 163–168.

Table 4. Selectivities and Sensitivities of Ionophores for Binding NH_4^+ over K^+ at pH 8.0

ionophores	selectivity ($\log K_{\text{NH}_4^+/\text{K}^+}$)	detection limit (M)
5	-2.8	1.0×10^{-4}
6	-2.3	2.5×10^{-5}
7	-1.7	2.0×10^{-4}
nonactin	-1.3	2.2×10^{-5}

the receptor (**6**) should reduce its basicity and decrease the concentration of the singly protonated form of the receptor relative to the neutral form at a given solution pH (Scheme 1). Such electronic tuning should favor the binding of NH_4^+ over H_2O . Second, increasing the solution pH should also decrease the singly protonated form of the receptor and increase the sensitivity of the receptor for binding NH_4^+ over H_2O . However, the solution pH should be kept below the $\text{p}K_a$ of NH_4^+ since ISEs are not responsive to NH_3 .

Figure 3a shows that with increasing solution pH, the sensitivity of **6** based ISEs approaches that of nonactin based ISEs (Figure 3b). The sensitivity of nonactin does not change significantly with changing pH. Receptor **6** is about equally sensitive as nonactin at pH 9 but the former is about 10 times more selective than the latter for binding NH_4^+ over K^+ (Table 4). It is interesting that the combination of three H-bonds and a cation- π interaction is enough for **6** to have comparable sensitivity as nonactin.

To dissect the steric and electronic effects of the methyl and bromo groups in **6**, we compared the selectivity and sensitivity of **6** to those of **5** and **7** for binding NH_4^+ . The basicity of the pyrazole groups in **6** is expected to be close to that in **7** since the $\text{p}K_b$ of 1-methylpyrazole (11.94) is comparable to that of 1,3,5-trimethyl-4-bromopyrazole (12.25).¹⁸ Thus the electronic effect of the pyrazoles in **7** should be similar to that in **6** and the steric effects of the methyl groups in **6** can be studied in isolation. The three methyl groups on the 3-position of the pyrazole rings in **6** were intended to increase the selectivity of the receptor for binding NH_4^+ over K^+ by blocking any ligands from coordinating to K^+ from the top. The crystal structure (Figure 2) of NH_4^+ bound to **6** reveals that the methyl groups on the 3-position of the pyrazoles shield the cation such that it would be difficult to form a 2:1 complex between the receptor and K^+ . This strategy appears to have worked since the selectivity of **6** is significantly greater than that of **7** for binding NH_4^+ over K^+ (Table 5). The three methyl groups on the 5-position of the pyrazole rings in **6** were placed to direct the three imine nitrogens inward for binding NH_4^+ . This preorganization effect is expected to increase the sensitivity of the receptor by increasing the equilibrium constant for binding NH_4^+ . This strategy also appears to have worked since the sensitivity of **6** for binding NH_4^+ is significantly greater than that of **7** (Table 4).

Just as we have been able to isolate the steric effects of the methyl groups in **6** it is possible to isolate the electronic effect of the bromo groups in the receptor. The steric effects of the methyl groups in receptors **6** and **5** should be similar but the electronic effects of the pyrazole groups in the two receptors are significantly different. The pyrazoles in **6** are expected to

be less basic than that in **5** since the $\text{p}K_b$ of 1,3,5-trimethyl-4-bromopyrazole (12.25) is significantly higher than that of 1,3,5-trimethylpyrazole (10.26).¹⁸ The more basic receptor should protonate more easily to form the water binding receptor (**5H**⁺, Scheme 1). Since NH_4^+ competes for the water binding site, the sensitivity of the more basic receptor for binding the cation is expected to be lower (Scheme 1). Indeed, **6** is more sensitive than **5** for binding NH_4^+ (Table 4). While **5** is less sensitive than **6**, it is somewhat more selective than **6** for binding NH_4^+ over K^+ (Table 4). Thus, it appears that the electron withdrawing group (Br) in **6** lowers the strength of the N-H-N hydrogen bonds more than the strength of the K-N bonds. In agreement with this experimental result, ab initio computation shows that **5** is more selective than **6** for binding NH_4^+ over K^+ .¹⁹

It is also interesting to compare the sensitivities and selectivities of **5** and **7** for binding NH_4^+ . While **5** is more selective than **7** for binding NH_4^+ over K^+ , the two receptors have comparable sensitivities for binding NH_4^+ (Table 4). As mentioned above for **6**, the three methyl groups on the 3-position of the pyrazole rings in **5** are expected to increase the selectivity of the receptor for binding NH_4^+ over K^+ by blocking any ligands from coordinating to K^+ from the top. The three methyl groups on the 5-position of the pyrazole rings in **5** are expected to increase the sensitivity of the receptor for binding NH_4^+ by converging the three imine nitrogens. However, the basicity of the pyrazoles in **5** is greater than that in **7** and this effect is expected to make **7** more sensitive (Scheme 1). Thus the electronic effect of the methyl groups in **5** is to decrease the sensitivity of the receptor while the steric effect of the methyl groups on the 5-position of the pyrazoles is to increase the sensitivity of the receptor and the two effects appear to cancel each other (Table 4).

In summary, an artificial receptor (**6**) based ISE is as sensitive (at pH 9) and 10 times more selective than nonactin based ISEs for sensing NH_4^+ over K^+ . Steric and electronic effects, as well as H-bonding and cation- π interactions, were taken into consideration in designing the receptor. The three pyrazole groups in **6** were designed to accept three H-bonds from NH_4^+ . The three ethyl groups in **6** were designed to direct the three pyrazole rings to the same side of the benzene ring by steric interactions.¹⁵ The three methyl groups on the 5-position of the pyrazole rings were designed to converge the imine nitrogen atoms for binding NH_4^+ by steric interactions and the three methyl groups on the 3-position of the pyrazole rings were designed to block ligands from coordinating to the top. The three electron withdrawing groups (Br) on the receptor were placed to increase the sensitivity of the receptor for binding NH_4^+ by decreasing the water binding form of the receptor (**6H**⁺). Finally, the benzene ring of the receptor is expected to stabilize NH_4^+ by cation- π interactions. The crystal data and

(19) Ab initio calculations were performed using the GAMESS program. Schmidt, M. W.; Baldridge, K. K.; Boatz, J. A.; Elbert, S. T.; Gordon, M. S.; Jensen, J. H.; Koseki, J. H.; Matsunaga, N.; Nguyen, K. A.; Su, S. J.; Windus, T. L.; Dupuis, M.; Montgomery, J. A. *J. Comput. Chem.* **1993**, *14*, 1347-1363. The geometries were fully optimized under the C_3 symmetry condition at the RHF/3-21G* level. The binding energies of the complexes were corrected for basis set superposition error (BSSE). BSSE is calculated by using the counterpoise method with a modification that takes into account the change in geometries upon complexation. Boys, S. F.; Bernaradi, F. *Mol. Phys.* **1970**, *19*, 553-566. Nagy, P. I.; Smith, D. A.; Alagona, G.; Ghio, C. *J. Phys. Chem.* **1994**, *98*, 486-493.

(18) Catalan, J.; Abboud, L. M.; Elguero, J. *Adv. Heterocycl. Chem.* **1987**, *41*, 187-274.

ISE data support our design rationale and can be used to quantitatively dissect the electronic and steric effects of the bromo and methyl substituents on the selectivity and sensitivity of **6** for binding NH_4^+ . The crystallographic investigation provides valuable insight into the origin of selective binding of the receptor to NH_4^+ over H_3O^+ . This receptor with its simple platform allows detailed understanding of NH_4^+ recognition, and it is ideally set up for molecular mechanics and ab initio computations.^{15,19} Fundamental information gained from the studies of NH_4^+ recognition may be helpful not only for sensing this cation but also for sensing other structurally related and biologically interesting compounds such as amino acids and the dopamine class of neurotransmitters.

Acknowledgment. We gratefully acknowledge the Creative Research Initiative Program of the Korean Ministry of Science and Technology and the Natural Sciences and Engineering Research Council of Canada for support of this work and the BK21 Program of the Korean Ministry of Education for a graduate fellowship to J.Oh. We also thank J. Heo for the crystal structures shown in Figures 1 and 2.

Supporting Information Available: Crystallographic information for $[\mathbf{5H}^+\cdot\text{H}_2\text{O}]\text{ClO}_4^-$ and $[\mathbf{6NH}_4^+]\text{PF}_6^-$ (PDF). This material is available free of charge via the Internet at <http://pubs.acs.org>.

JA0174175